View metadata, citation and similar papers at core.ac.uk

brought to you by CORE

provided by Elsevier - Publisher Connector

Computational Condensed Matter 1 (2014) 32–37

Contents lists available at ScienceDirect

Computational Condensed Matter

journal homepage: http://ees.elsevier.com/cocom/default.asp

Regular article

Physical properties of RbAu compound

Murat Aycibin*, Emel Kilit Dogan, Sinem E. Gulebaglan, M. Nurullah Secuk, Bahattin Erdinc, Harun Akkus

Department of Physics, Faculty of Science, Yuzuncu Yil University, 65080 Van, Turkey

ARTICLE INFO

Article history:
Received 5 September 2014
Received in revised form
9 October 2014
Accepted 9 October 2014
Available online 8 November 2014

Keywords:
Electronic structure
Semiconductors
Thermo-dynamic properties
Optic properties
Ab initio calculations

ABSTRACT

In this paper, we investigated electronic, optic, elastic, dynamic and thermodynamic properties of RbAu compound by density functional theory within the generalized gradient approximation. The calculated static value of real part of dielectric constant is 6.7. The calculated electronic band structure of RbAu shows that RbAu is a semiconductor with an indirect band gap of 0.36 eV. Besides, RbAu obeys mechanical stability and it demonstrates elastic anisotropy. 540K is classical limit for specific heat of RbAu.
© 2014 The Authors. Published by Elsevier B.V. This is an open access article under the CC BY-NC-ND license (http://creativecommons.org/licenses/by-nc-nd/3.0/).

1. Introduction

Molecules and solids containing intermetallic bonds of the late transition metals have been studied by numerous scientists including chemists, physicists and engineers for more than half a century. A group of these compounds includes alkali (Li, Na, K, Rb, Cs) and noble metals (Cu, Ag, and Au). Due to the potential use of gold compounds in the field of microelectronics, catalysis, medical, biology, nanostructure materials and optic, intermetallic compounds including gold are widely investigated [1]. Gold is of interest because it is the only metal forming a simple isolable monoatomic anion. Due to the electronic configuration of gold, its compounds are relatively stable [2]. After discovery of the CsAu and RbAu, the nature of intermetallic bonds between alkali metals and gold was subject to various experimental and theoretical studies [3–13].

Norris and Wallden performed the photoemission spectra measurement on MAu (M = Cs, Rb) and they concluded that RbAu is metallic [3]. Belpassi et al. studied and calculated the spectroscopic constants such as dissociation energy, harmonic and an harmonic vibrational frequencies and dipole moments for all alkali auride series [4]. Koenig et al. performed the relativistic band-structure calculation of alkali-metal gold compounds [5]. Liu investigated electronic and optic properties of RbAu and CsAu compounds using some well-known formulas from optics [6]. Grosch and Range calculated the structural properties of MAu alloys (M = Li, Na, K, Cs, Rb) and examined the electronic valance charge densities of these compounds [7]. Yu et al. used first principle method based on the density function theory (DFT) to calculate the structural and elastic properties of RbAu [8]. Tinelli and Holcomb performed NMR and X-Ray measurement of RbAu and CsAu and investigated the structural properties of these compounds [9]. Overhof et al. obtained the photoemission data of polycrystalline RbAu and CsAu [10]. Huang and Liu presented the electronic energy bands of MAu (M = Cs, Rb, Li) [11].

Some works dealt with more complex structure of alkali auride series. Hu et al. investigated Au_nRb for different n values and analyzed the geometric structure, growth pattern behavior and electronic properties [12]. Klepp and Weithaler determined the crystal structure of $RbAu_3Se_2$ and found out its characteristic properties [13]. Meloni and Baldercschi used the self-consistent local density pseudo potential method to calculate the energy band structures of RbAu and KAu. Moreover, they also investigated $K_xRb_{1-x}Au$ within the virtual crystal approximation [14].

Based on our best knowledge, a comprehensive study on the physical properties of RbAu has not been carried out yet. Therefore, in this paper, we have performed the first-principle calculations to investigate the physical properties of RbAu compound to see whether it is a semiconductor or not.

* Corresponding author.
E-mail address: murataycibin@yyu.edu.tr (M. Aycibin).

http://dx.doi.org/10.1016/j.cocom.2014.10.004
2352-2143/© 2014 The Authors. Published by Elsevier B.V. This is an open access article under the CC BY-NC-ND license (http://creativecommons.org/licenses/by-nc-nd/3.0/).

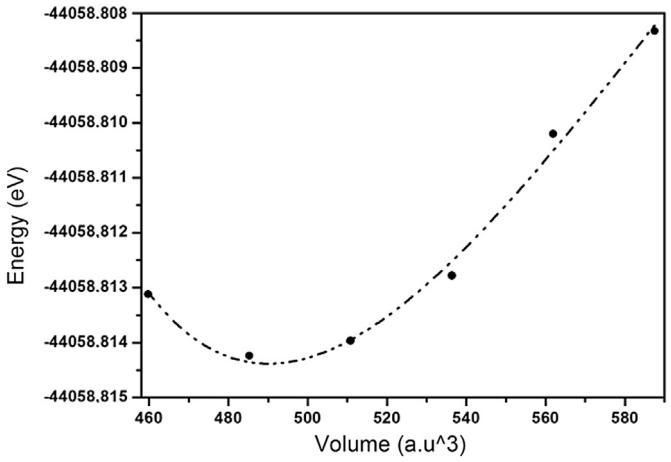

Fig. 1. Dependence of total energy on unit cell volume for cubic RbAu.

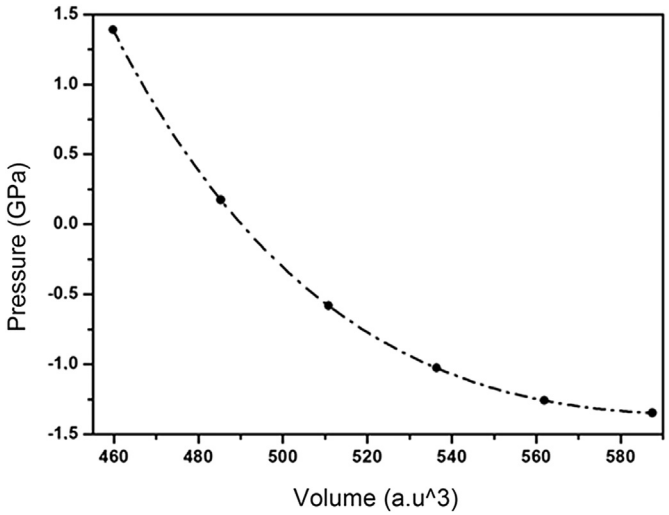

Fig. 2. Pressure versus volume for RbAu.

2. Computational methods

The physical properties of RbAu have been investigated using both ABINIT [15] and WIEN2K codes [16]. The full potential linearized augmented plane-wave (FP-LAPW) method [17] with Perdew–Burke–Enzerhof (PBE) [18] generalized gradient approximation (GGA) functional is used to solve Kohn–Sham equations. While ABINIT package was used to calculate the dynamic and thermodynamic properties, WIEN2K package was used to obtain the structural, electronic and optic properties of RbAu compound. 286k points were used in the first Brilliouin zone (BZ) for the structural, electronic and optic properties. For the dynamic and thermodynamic calculations, energy cutoff was taken 30 Hartree for good convergence, after careful optimization, 56 K points used to construct a 12 × 12 × 12 Monkhorst–Pack mesh grid (MPMG) [19]. In the calculations, the $5s^1$ and $4f^{14}5d^{10}6s^1$ electrons were considered as the true valence for Rb and Au atoms, respectively.

3. Structural properties

The RbAu has a simple cubic structure with 2 atoms per unit cell and crystallizes in the CsCl-type structure [20] with space group *Pm-3m*. The calculations have been performed by considering Rb atom is centered at (0, 0, 0) and Au atom is located at (0.5, 0.5, 0.5) in the reduced coordinates. The volume of unit cell is optimized using WIEN2K code. The total energy of RbAu compound has been calculated as a function of the unit cell volume and fitted to the Birch–Murnaghan equation of state [21] in Fig. 1. This is used to determine ground state properties such as equilibrium lattice constant, unit cell volume, bulk modulus and the pressure derivative of the bulk modulus. The obtained results are given in Table 1.

Calculated lattice constant a_0, Bulk modulus B_0 (in GPa) and its pressure derivative $B_0^{'}$ (in GPa) for RbAu comparing with available experimental result.

In Fig. 1, it is seen that the minimum value of energy, −44,058.81 eV, corresponds to the ground state volume with value of 490.18 $(a.u)^3$. Therefore, the calculated lattice constant for RbAu is found 4.17 Å. Meanwhile, the experimental value of lattice constant is 4.10 Å [20]. If we compare theoretical lattice constant with experimental one, experimental lattice constant is shorter as a result of GGA-type functions. The pressure versus volume is given in Fig. 2. It can be extracted from the figure that zero pressure value corresponds to minimum volume value, about 490 $(a.u)^3$, where minimum total energy is obtained. In other words, total net force acting on atoms equals to zero at minimum total energy.

Table 1
Calculated lattice constant a_0, Bulk modulus B_0 (in GPa) and its pressure derivative $B_0^{'}$ (in GPa) for RbAu comparing with available experimental result.

Parameter	a_0 (in Å)	B_0	$B^{'}$
RbAu	4.17 4.10[a]	16.75	8.246

[a] See [20].

4. Electronic properties

The band structure of RbAu has been studied both theoretically and experimentally using various techniques [3–6,9–11]. According to these works, RbAu was classified either metal [3,9] or narrow-band semiconductor [4,5,14]. In the present work, the calculated band structure for RbAu is given in Fig. 3 where Fermi energy level was set to origin and shown with dashed line. Top of valence band is located at the high symmetry point R while the bottom of conduction band is located between the high symmetry points Γ and X in the BZ, therefore, RbAu has an indirect band gap

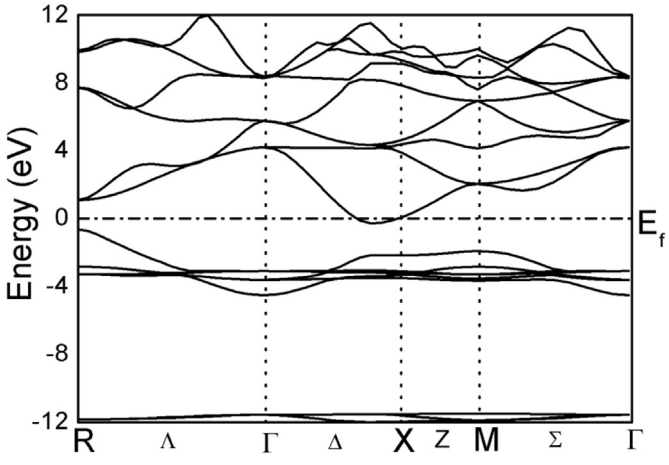

Fig. 3. Calculated electronic band structure of RbAu.

with value of 0.34 eV. The calculated band structure is in good agreement with previous works [5,10].

Density of state (DOS) for RbAu is calculated and given in Fig. 4. One can see that main contribution to the top valence band comes from Au atoms and Rb atom mainly contributes to the deep valence band. However, contribution of $6s^1$ state of Au atom and Rb atom to the top valence band is negligible.

5. Optic properties

Since RbAu has cubic symmetry, it is only needed to calculate one dielectric component. 0–40 eV photon energy range is sufficient to calculate optic response of RbAu. The calculated real and imaginary parts of dielectric constant are given in Fig. 5. As seen in Fig. 5, the static values of real part of dielectric constant, $\varepsilon_1(0)$, is 6.7 which is different from the value of real part of dielectric constant given in a previous work [6]. There is no absorption till 0.34 eV. After this point, optic transitions from valance band to conduction band can be observed. In addition, $\varepsilon_1(\omega)$ becomes zero at some certain energy values and then decrease to minimum values below the zero energy level at 3.75, 8.15 and 21.62 eV. The negative values of $\varepsilon_1(\omega)$ means that in this regions, the incident electromagnetic waves are entirely reflected. After the third negative values of real part of dielectric constant, $\varepsilon_1(\omega)$ gets closer to zero values, which means there is no transition between states (over 23 eV).

According to a previous work [6], the imaginary part of dielectric function has a maximum at 2.37 eV photon energy value, but our calculations display a maximum peak at 3.28 eV photon energy value corresponding strong optic transitions.

Fig. 6 shows results for reflectivity R, refractive index n, extinction coefficient k and energy loss function L. The function L for volume shown in Fig. 6d describes the energy loss of a fast electron traversing the material. As shown in the figure, sharp peaks are associated with plasma oscillations corresponding to the photon energy values, where the real part of dielectric constant becomes zero. These peak values are 9.08, 24.34, 29.53 and 33.26 eV.

6. Elastic constant

To obtain elastic constants of this compound, we used the method developed by Morteza Jamal integrated in WIEN2K code [22]. Due to cubic structure, only three independent elastic

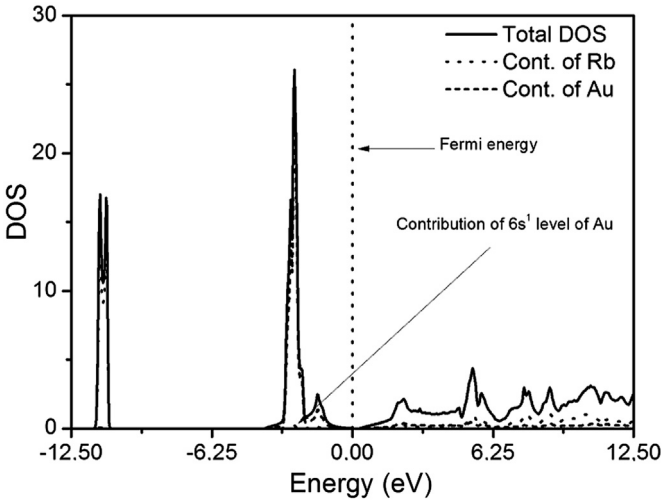

Fig. 4. Calculated total and partial DOSs for RbAu.

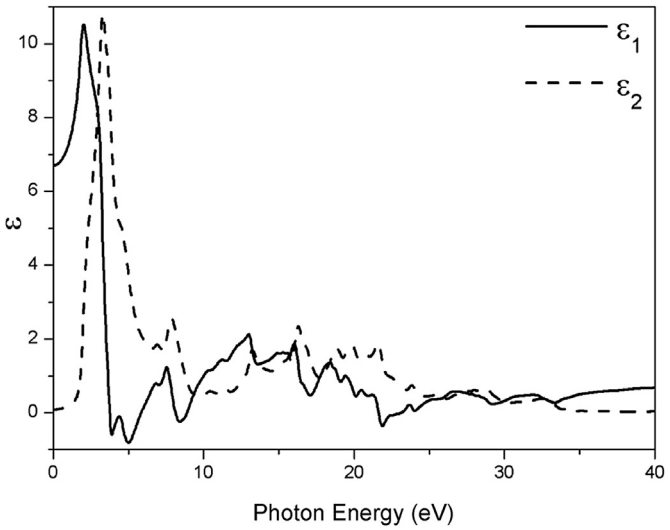

Fig. 5. Real (ε_1) and imaginary (ε_2) parts of dielectric constant for cubic RbAu.

constants, namely C_{11}, C_{12} , and C_{44}, are required to completely account for elastic properties. We calculated young module, shear modulus, bulk modulus, and poisson's coefficients with three different approximations that are Voight, Reuss and Hill using the mentioned method [23]. Besides, anisotropy ratio (A) and compressibility were calculated with these three elastic constants. All of the calculated quantities at 0 GPa are given in Table 2. Unfortunately, there is currently no experimental data for elastic constants of this compound to compare.

Calculated single crystal elastic constants (C_{ij} in GPa), Bulk modulus (B_0 in GPa), anisotropy factor (A), compressibility (β in GPa^{-1}), Young Modulus (E) and Shear Modulus (G) obtained for RbAu.

Bulk modulus was calculated both using total energy-volume data in Table 1 and Jamal methods in Table 2. Comparing these two results, we concluded that the measurement of the predicted result is reliable.

The anisotropy factor (A) was calculated in order to provide insight on the elastic anisotropy of these materials. The values shown in Table 2 are clearly less than a value of one that indicates complete isotropy. The anisotropy value of this compound is 0.796, which suggest that RbAu compound exhibits elastic anisotropy.

Analyzing these three elastic constants, we saw that the elastic constants of RbAu crystal obey the mechanical stability criteria of the cubic structure [24,25] namely,

$$C_{11} - C_{12} > 0,\ \ C_{11} > 0,\ \ C_{44} > 0 \ \text{ and } \ C_{11} + 2C_{12} > 0$$

This confirms that RbAu compound is mechanically stable which implies that the strain energy must be positive. Moreover, the values of C_{11} is far larger than C_{12} and C_{44} which indicates some significant resistance to pure shear deformations by the compounds [24].

7. Thermodynamical and dynamical properties

RbAu crystal has 2 atoms per unit cell. Rb atom is located at (0, 0, 0) and Au atom is at (0.5, 0.5, 0.5). Ab initio calculation of the phonon band structure was explained in details [15,26]. For two atoms per unit cell, we have six phonon branches, three of them are acoustic modes and the remaining are optic modes. The calculated phonon dispersion curves along Γ-X-M-Γ-R-X-M-R directions are displayed in Fig. 7, where there is a gap between the optic and acoustic modes. Some of the branches are degenerate along more

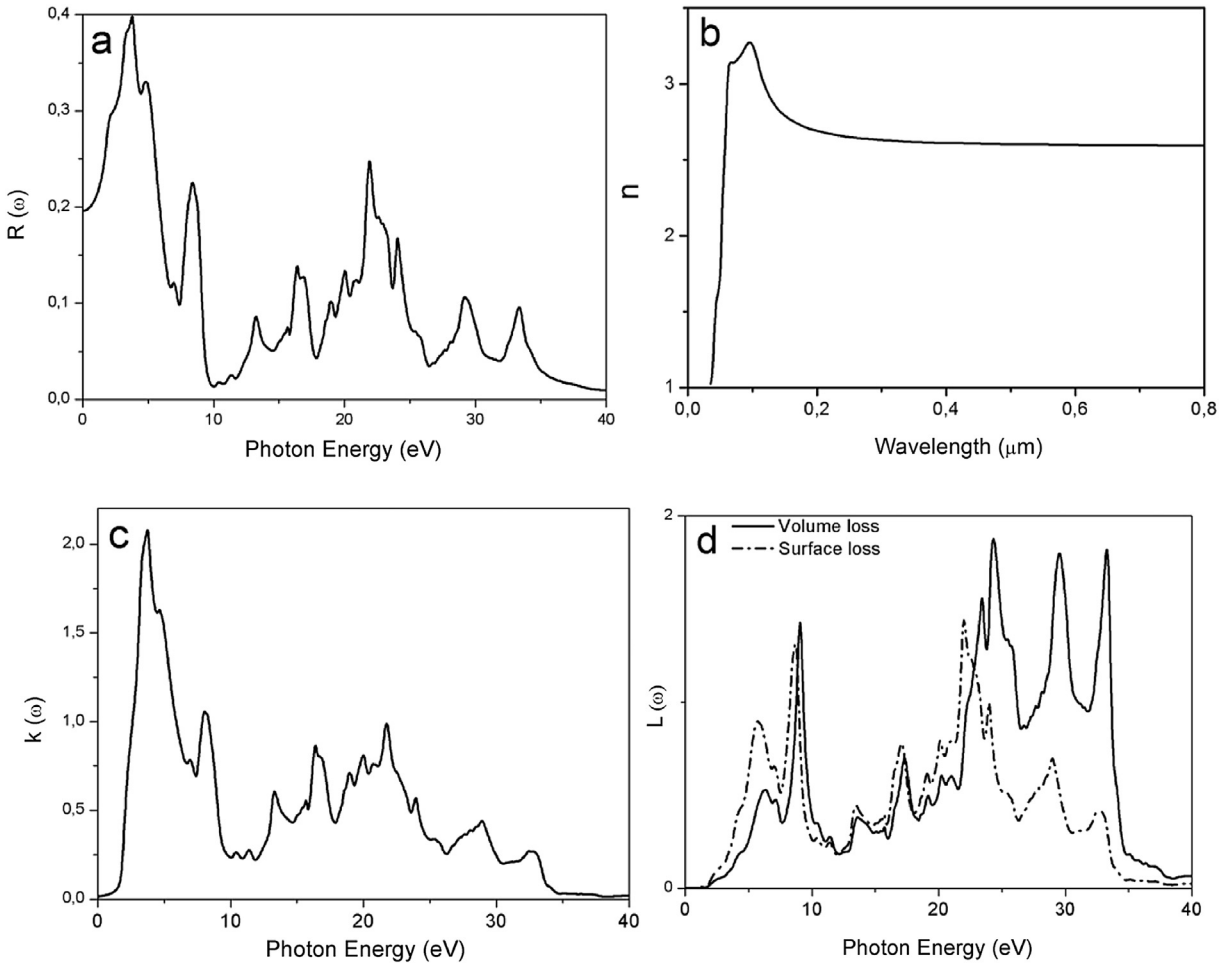

Fig. 6. Optical constants for RbAu.

symmetrical directions inside the BZ of RbAu crystal. The direction Δ, which is from Γ to *X*, Λ which is from Γ to R, and T which is from M to R are more symmetrical than the other symmetry directions. At these more symmetrical directions, transverse optical (TO) and acoustical (TA) modes are degenerate. When symmetry is broken along the other directions, degeneracy disappears in these modes. One can see from Fig. 7 that the acoustic phonon dispersion curves are linear function of k for small k values at around Γ high symmetry point. The values of calculated frequency of TO and longitudinal optical (LO) are 23.47 and 28.14 THz at the center of BZ, respectively. Moreover, TO has degeneracy at the center of BZ. We are not able to compare our dynamic data with any experimental or theoretical work due to lack of both in literature.

A factor group analysis of phonon modes at the zone center based on the group theory has been carried out using the Bilbao Crystallographic Server [27] for RbAu crystal structures with space group number 221. Acoustic and optic modes have T_{1u} symmetry. Optically active modes are in infrared region (IR) and there is no Raman active mode.

The obtained frequency values of the modes are 12.67 THz (LA), 13.10 THz (TA), 19.10 THz (TO) and 30.32 THz (LO) at the *X* high symmetry point, while 5.73 THz (LA), 12.70 THz (TA), 18.70 THz (TO) and 26.03 THz (LO) at the M high symmetry point. As seen from Fig. 7, LA modes intersect with one of TA modes four times at points of $k = 2\pi/a$ (0.333, 0.333, 0), $k = 2\pi/a$ (0.333, 0.333, 0.333), $k = 2\pi/a$ (0.1, 0.5, 0.1) and $k = 2\pi/a$ (0.1167, 0.5, 0). Moreover, LO modes intersect with one of TO modes 3 times at points of $k = 2\pi/a$ (0.25, 0.25, 0), $k = 2\pi/a$ (0.02, 0.02, 0.02) and $k = 2\pi/a$ (0.3, 0.3, 0.3).

Various thermodynamic properties of a solid can be extracted from calculated phonon DOS. The entropy (S), constant-volume specific heat (C_v), the phonon contributions to Helmholtz free energy (F), and internal energy (E) as a function of temperature for RbAu are given in Fig. 8. The contribution of phonon to the internal and free energies is calculated and it is seen from the figure that the contributions of lattice do not vanish at zero temperature. The contribution of phonon to internal energy (ΔE_0), and free energy (ΔF_0), are the same, that is, 0.95 J/mole at absolute zero temperature (see Fig. 8c and d). That means zero-point oscillations manifest themselves. The temperature dependent entropy is also calculated from phonon band structure calculations. One can see in Fig. 8a entropy curves as a function of the temperature. Finally, constant-volume specific heat for RbAu is given in Fig. 8b, in which the specific heat (C_V) approaches to its classical limit value at 540 K.

Table 2
Calculated single crystal elastic constants (C_{ij} in GPa), Bulk modulus (B_0 in GPa), anisotropy factor (A), compressibility (β in GPa^{-1}), Young Modulus (E) and Shear Modulus (G) obtained for RbAu.

Parameter	C_{11}	C_{12}	C_{44}	B_0[a] (GPa)	E[a] (GPa)	G[a] (GPa)	P	A	β
RbAu	25.52	9.55	6.36					0.796	0.067
VOIGHT				14.87	7.01	18.17	0.296		
REUSS				14.87	6.92	17.98	0.298		
HILL				14.87	6.97	18.08	0.297		

[a] See ref [4].

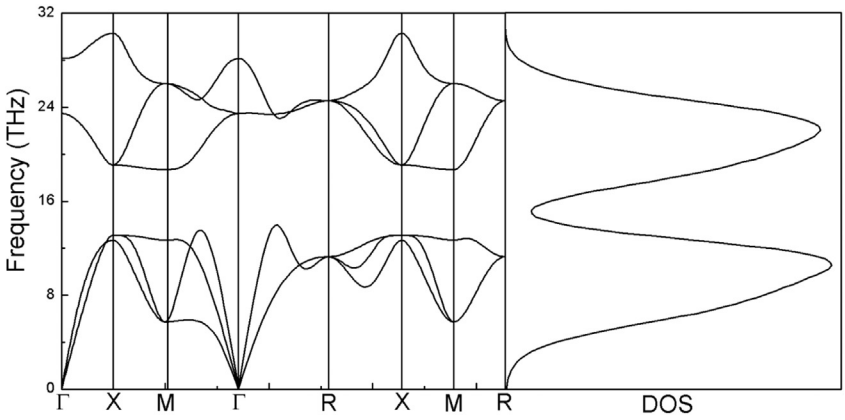

Fig. 7. Phonon dispersion curves and phonon density of states for RbAu.

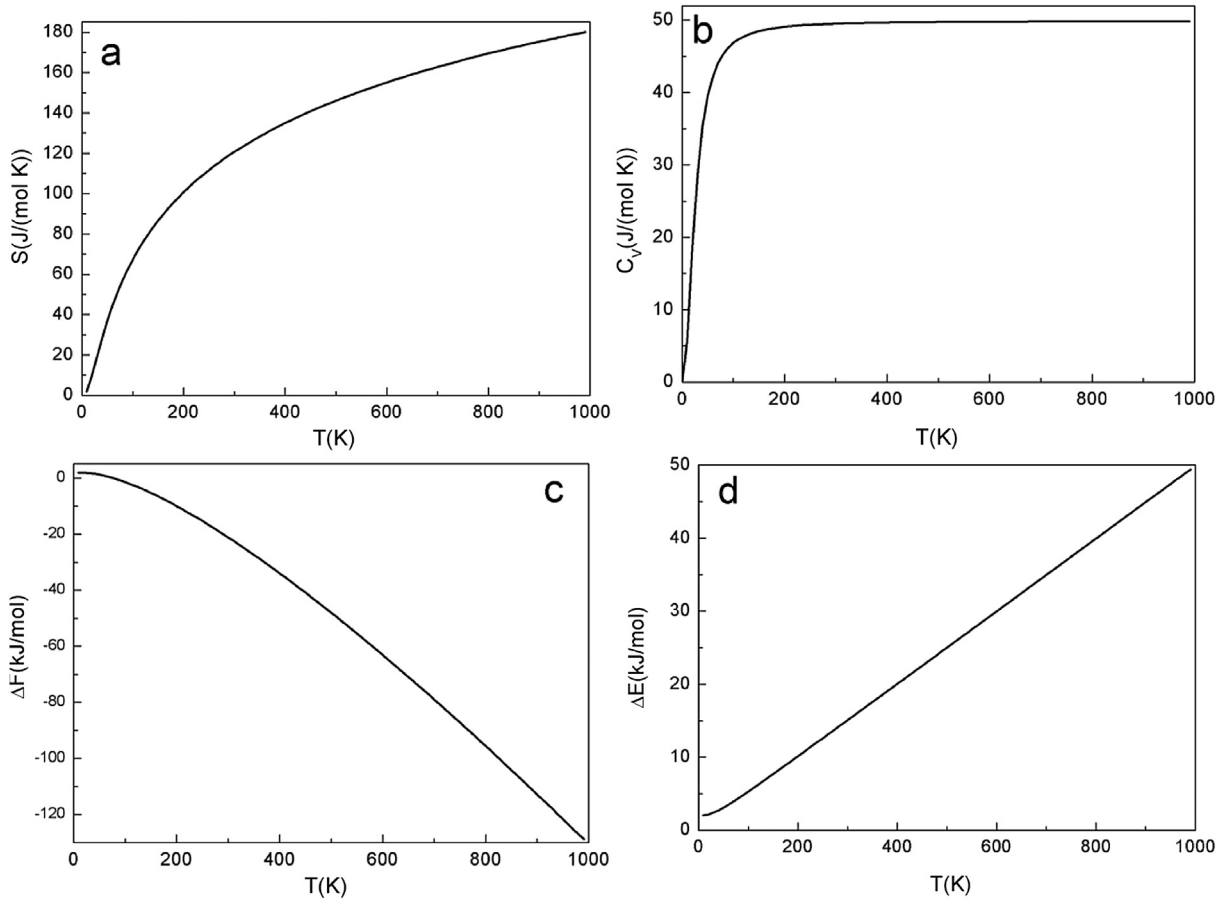

Fig. 8. (a) The entropy as a function of temperature, and (b) constant–volume specific heat as a function of temperature, (c) Phonon contribution to the free energy as a function of temperature, (d) Phonon contribution to the internal energy as a function of temperature for RbAu.

8. Conclusion

In this paper, we have investigated electronic, optic, dynamic and thermodynamic properties of RbAu using WIEN2K and ABINIT codes. GGA was used for exchange and correlation effects. The obtained lattice constant is consistent with the experimental results. According to our calculations, the RbAu can be classified as a semiconductor with a narrow band gap and it has indirect transition. RbAu obeys mechanical stability criteria and demonstrate elastic anisotropy.

Acknowledgments

This work has been supported by the Unit of Scientific Research Projects of Yuzuncu Yil University under project No. 2011-FED-B010.

References

[1] K.O. Klepp, C. Weithaler, J. Alloys Compd. 243 (1996) 1–5.
[2] A. Laguna, Modern Supramolecular Gold Chemistry: Gold-metal Interactions and Applications, Wiley-VCH, John Wiley distributor, Weinheim, Chichester, 2008.

[3] C.A. W, L. Norris, Phys. Status Solidi (a) 2 (1970).
[4] L. Belpassi, F. Tarantelli, A. Sgamellotti, H.M. Quiney, J. Phys. Chem. A 110 (2006) 4543–4554.
[5] C. Koenig, N.E. Christensen, J. Kollar, Phys. Rev. B 29 (1984) 6481–6488.
[6] T.L. Liu, Phys. Rev. B 12 (1975).
[7] G.H. Grosch, K.J. Range, J. Alloys Compd. 233 (1996) 30–38.
[8] Z.H. Yu, C.Y. Li, H.Z. Liu, Phys. B 407 (2012) 805–807.
[9] G.A. Tinelli, D.F. Holcomb, J. Solid State Chem. 25 (1978) 157–168.
[10] J.K.H. Overhoft, R. Fischer, F. Hemel, J. Phys. F. Met. Phys. 8 (1978).
[11] H.M. Huang, T.L. Liu, Phys. Lett. 46A (1973) 295–296.
[12] Y.F. Hu, F.J. Kong, S.J. Wang, Y.Q. Yuan, L.P. Jin, J. Mol. Struct. 1035 (2013) 165–173.
[13] K.O. Klepp, C. Weithaler, J. Alloys Compd. 243 (1996) 12–18.
[14] F. Meloni, A. Baldereschi, Lect. Notes Phys. 152 (1982) 43–48.
[15] X. Gonze, J.M. Beuken, R. Caracas, F. Detraux, M. Fuchs, G.M. Rignanese, L. Sindic, M. Verstraete, G. Zerah, F. Jollet, M. Torrent, A. Roy, M. Mikami, P. Ghosez, J.Y. Raty, D.C. Allan, Comput. Mater. Sci. 25 (2002) 478–492.
[16] K.S. P. Blaha, G.K.H. Madsen, D. Kvasnicka, J. Luitz, (2001).
[17] O.K. Andersen, Phys. Rev. B 12 (1975).
[18] J.P. Perdew, K. Burke, M. Ernzerhof, Phys. Rev. Lett. 77 (1996) 3865–3868.
[19] H.J. Monkhorst, J.D. Pack, Phys. Rev. B 13 (1976) 5188.
[20] A. Hasegawa, M. Watabe, J. Phys. F. Met. Phys. 7 (1977) 75.
[21] V.N. Belomestnykh, Tech. Phys. Lett. 30 (2004) 91–93.
[22] M. Jamal, (2012).
[23] M.J. Mehl, B.M. Klein, D.A. Papaconstantopoulos, R.L. F.E, J.H. Westbrook, Intermediate Compounds: Principles and Practice, John Wiley and Sons, London, 1994.
[24] J.F. Nye, Physical Properties of Crystal: Their Representation by Tensor and Matrices, Oxford University Press, Oxford, 1985.
[25] M.L. Cohen, Phys. Rev. B 32 (1985) 7988–7991.
[26] C. Lee, X. Gonze, Phys. Rev. B 51 (1995) 8610–8613.
[27] M.I. Aroyo, J.M. Perez-Mato, D. Orobengoa, E. Tasci, G. de la Flor, A. Kirov, Bulg. Chem. Commun. 43 (2011) 183–197.